Magnetospirillum magneticum as a living iron chelator induces transferrin receptor 1 upregulation in cancer cells

Stefano Menghini†, Ping Shu Ho†, Tinotenda Gwisai, Simone Schuerle*

Institute for Translational Medicine, Department of Health Sciences and Technology,
ETH Zurich, CH-8092 Zurich, Switzerland.

Abstract

Iron chelating agents derived from bacterial siderophores were originally used for iron overload syndromes but have recently been investigated for cancer therapy. While systemic administration of iron chelating agents induces undesirable side effects, bacteria as a source of siderophores could potentially act as local chelator that is tumor-targeted and amplifies its impact through preferential accumulation and self-replication in tumors. Here, we report the use and characterization of *Magnetospirillum magneticum* AMB-1 as living iron chelator. We quantified the amount of secreted bacterial siderophores and show that they exert changes in human transferrin's (Tf) structure. Next, we examined the bacteria's ability to target iron homeostasis *in vitro* and our experiments revealed an increased expression of transferrin receptor 1 (TfR1). Our results suggest that magnetotactic bacteria have potential as self-replicating antineoplastic agents which compete with cancer cells for iron, and might be a solution for overcoming challenges of current iron chelation cancer therapies.

† These authors contributed equally

* Corresponding author: simone.schuerle@hest.ethz.ch

Introduction

Iron is an essential nutrient required for numerous mammalian cell functions, and plays a crucial role in cancer development and progression.[1, 2] Iron metabolism is significantly altered in mammalian tumor cells and, as such, is a metabolic hallmark of cancer.[3, 4] The main iron uptake mechanism adopted by most cells utilizes the internalization of transferrin receptor 1 (TfR1) upon binding of iron-bound transferrin (Tf). TfR1 expression positively correlates with cellular iron starvation and is upregulated in cancer cells, since malignant cells generally require an iron surplus, especially for proliferation and spread.[4-6]

Bacteria and other microorganisms secrete siderophores, natural iron chelators that display a greater affinity for iron than proteins secreted by eukaryotic cells, such as transferrin. These highly selective and potent microbial iron chelators are released in a pathogenic context, allowing bacteria to out-compete the host cells for ferric iron.[7, 8] Deferoxamine (DFO), a siderophore isolated from *Streptomyces pilosus*, is a natural iron chelator used to treat syndromes characterized by excess iron in the body such as hemochromatosis.[9, 10] Synthetic iron-chelators with enhanced pharmacologic and pharmacokinetic properties have also been developed.[11] Deferasirox is an FDA approved synthetic oral chelator used in the treatment of transfusion iron overload conditions. Recently, it was found to induce a significant decrease in tumor cell viability in both *in vitro* and *in vivo* studies.[12-14] Both natural and synthetic iron-chelators have been utilized to compete with malignant cells for available iron sources and several have demonstrated significant anti-neoplastic activity. However, non-negligible side effects, systemic toxicity, and low efficacy have hampered their translation into clinical trials as therapeutic agents for cancer treatment.[15-17]

Gram-negative magnetotactic bacteria (MTB) secrete high-affinity siderophores and use the acquired iron for both survival and synthesis of magnetite.[18, 19] The biomineralized magnetite nanocrystals are arranged in chains enclosed in a lipid bilayer and these intracellular organelles, called magnetosomes, enable them to align along magnetic fields.[20-22] Furthermore, MTB are aerotactic, possessing an oxygen-sensing system that regulates motility in an oxygen gradient.[23, 24] Aerotaxis and hypoxic traits have been leveraged in *Salmonella* strains, enabling them to act as bacterial anti-cancer agents that target necrotic tumor microenvironments with poor oxygen supply.[25, 26] In addition to enhanced tumor accumulation, native bacterial cytotoxicity, expression of anticancer agents, and localized gene-triggering systems have been exploited for their use in clinical cancer therapy.[27-30]

Here, we report the potential of localized iron deprivation as another weapon in bacterial cancer therapy by employing *Magnetospirillum magneticum* AMB-1. Like other magnetotactic bacteria, AMB-1 endogenously biomineralizes magnetosomes through the uptake of iron from their environment.[22, 31] We investigated the effect of AMB-1 produced siderophores on human transferrin structure and, thus, their potential as iron chelation agents. Additionally, we studied the influence of AMB-1 siderophores on cell surface TfR1 expression using human melanoma cancer cells. Exploiting the iron scavenging

properties of magnetotactic bacteria in combination with their ability to be used as bacterial anti-cancer agents may enable AMB-1 to be implemented for anti-neoplastic purposes.

Results

AMB-1 produced siderophores affect human transferrin structure in mammalian cell culture medium

First, we sought to determine whether AMB-1 would produce siderophores in Dulbecco's Modified Eagle's medium (DMEM). Using the Chrome Azurol S (CAS) assay (Supplementary Fig. 1), 10^8 AMB-1 cells were found to produce 0.10 ± 0.005 siderophore units in DMEM supplemented with 25 μM holo-transferrin (holo-Tf), while siderophore production in transferrin-free DMEM was negligible (Fig. 1A). AMB-1 siderophore production was compared to the widely used iron chelator deferoxamine. It was found that the siderophores produced by 10^8 AMB-1 in Tf-supplemented media was equivalent to 3.78 μM ± 0.117 μM deferoxamine (Fig. 1B).

Having established the ability of AMB-1 to produce siderophores in Tf-supplemented media, we next determined whether AMB-1 would have an effect on human transferrin structure. SDS-PAGE analysis was used to compare DMEM supplemented with either iron-containing holo-Tf or iron-depleted apo-Tf. The apo-Tf appeared as a broader band on the SDS-gel compared to holo-Tf (Fig. 1C). Furthermore, we ascertained that holo-Tf structure was not affected by a 48 h incubation period at 30°C. To test whether the bacteria induced changes in Tf, AMB-1 were inoculated in DMEM supplemented with holo-Tf. This approach revealed that holo-Tf formed a broader band very similar to that seen for the apo-Tf band incubated in DMEM (Fig. 1C, lane 6). These experiments demonstrate that AMB-1 produced a quantifiable amount of siderophore when holo-Tf was supplemented to the mammalian cell culture media and that the structure of holo-Tf was altered by the bacteria.

AMB-1 upregulates TfR1 expression in human melanoma cells

To determine whether AMB-1 can affect the iron uptake machinery in mammalian tumor cells we co-cultured AMB-1 with the human melanoma cell line MDA-MB-435S and monitored TfR1 expression using immunofluorescence. The surface expression of TfR1 increased 2.7-fold on cancer cells co-cultured with live bacteria at AMB-1:MDA-MB-435S ratios as low as 10:1 (10^6 AMB-1). The TfR1 upregulation was shown to increase with increasing bacteria ratios (Fig. 2A, B). Deferoxamine was used here to create iron-deficient cell culture conditions as a positive control. MDA-MB-435S cells showed a significant and increasing upregulation of TfR1 surface expression up to 5.6-fold. To ensure that the upregulation of TfR1 expression was on the cell surface and not cytoplasmic, cell membrane integrity in the cultures was monitored. Less than 5% of cells were stained by the cell-impermeant DNA stain propidium iodide (PI), indicating cell membrane preservation over time (Fig. 2C).

To gain insights on the TfR1 expression kinetics of the cell population, AMB-1-induced increase of cell surface TfR1 expression was analyzed over time. The effect, at an AMB-1:MDA-MB-435S ratio of 1000:1 was already apparent after 6 h of co-culture (Fig. 1D). The fluorescent intensity after 24 h of co-culture was 1.8 times higher than the initial value, while the change reached 95% of the final value after 12 h (Fig. 1E). Untreated cancer cells did not display any increase in fluorescence (Fig. 1F). Altogether, these findings show an upregulation of TfR1 on the cell surface of human melanoma cancer cells in presence of AMB-1, thereby suggesting a direct link between AMB-1 induced disruption of iron uptake and TfR1 expression.

Discussion

Magnetotactic bacteria acquire iron through siderophore-mediated uptake, as ferric and ferrous ions cannot enter bacteria cells directly. We quantified the amount of siderophores produced by strain *Magnetospirillum magneticum* AMB-1 and investigated the bacteria's effect on human transferrin's structure in mammalian cell culture medium. The addition of AMB-1 to the media led to a broader holo-Tf band, similar to the one of apo-Tf in DMEM, suggesting that the bacteria induced changes in Tf's molecular mass and structure (Fig. 1C, lane 6). Comparing our findings to studies involving the proteolytic cleavage of transferrin by *Prevotella nigrescens* we can deduce that specific cleavage of the protein did not occur, as sub-products with lower molecular mass were not detected on the gel.[32] Therefore, our results suggest a loss of iron ions by holo-Tf, which is consistent with bacteria-produced siderophores having a higher affinity for Fe ions compared to human transferrin.[7, 8] This higher affinity could be exploited by AMB-1 to efficiently compete for ferric ions with the host cells, resulting in iron starvation for the latter.

We then showed that AMB-1 inoculation with mammalian cancer cell cultures did affect iron homeostasis of the cancer cells. Increased TfR1 surface expression found on MDA-MB-435S melanoma cancer cells correlates with increasing bacteria ratios. This finding suggests that AMB-1 effectively competes for free iron ions and therefore limits the mineral's availability to MDA-MB-435S cells (Fig. 2A, B). Moreover, a significant increase of TfR1 expression could already be detected 6 h after inoculation (Fig. 2D-F). Similarly, the cancer cells showed a significant upregulation of TfR1 surface expression after incubation with deferoxamine (10 µM and 25 µM), in line with previous reports on cellular iron deficiency.[4, 5, 33] These observations demonstrated that AMB-1 affect the iron import mechanisms of human melanoma cells, acting as an effective competitor for iron when in co-culture with MDA-MB-435S cells.

Our data supports the idea that AMB-1 have the ability to act as living iron chelators by secreting a considerable amount of siderophores that was quantified. We showed that 10^8 AMB-1 are able to produce high-affinity iron scavenging molecules equivalent to 3.78 µM deferoxamine over 24 h (Fig.

1B). Previous studies demonstrated that the treatment of different cell lines with 10 µM - 30 µM deferoxamine significantly reduced cell viability *in vitro.*[13, 33] Moreover, significant diminution of cell viability was even detected at the lower deferoxamine concentration of 2.5 µM when combined with the chemotherapeutic drug cisplatin.[13] The ability of AMB-1 to self-replicate and secrete comparable, sustained doses of siderophores qualifies them as promising candidates for further studies.

The investigation of nutrient deprivation as a potential anti-cancer therapy is still in its infancy. Our work motivates the use of living AMB-1 as self-replicating iron chelators actively competing for this vital mineral, with the possibility of compromising the survival of cancer cells. This approach lays the foundation for future investigations which combine iron chelation with bacterial cancer therapy to enhance existing therapeutic strategies and open new frontiers for combating cancer.

Materials and Methods

Bacterial strain and culture condition

Magnetospirillum magneticum AMB-1, a strain of magnetotactic bacteria, was purchased from ATCC (ATCC, Manassas, Virginia, USA). AMB-1 bacteria were grown anaerobically at 30°C, passaged weekly and cultured in liquid growth medium (ATCC medium: 1653 Revised Magnetic Spirillum Growth Medium). *Magnetospirillum magneticum* Growth Media (MSGM) contained the following per liter: 5.0 mL Wolfe's mineral solution (ATCC, Manassas, Virginia, USA), 0.45 mL Resazurin, 0.68 g of monopotassium phosphate, 0.12 g of sodium nitrate, 0.035 g of ascorbic acid, 0.37 g of tartaric acid, 0.37 g of succinic acid and 0.05 sodium acetate. The pH of the media was adjusted to 6.75 with sodium hydroxide (NaOH) and then sterilized by autoclaving at 121°C. 10 mM ferric quinate (200x) Wolfe's Vitamin Solution (100x) (ATCC, Manassas, Virginia, USA) were added to the culture media shortly before use. The concentration of AMB-1 in solution was determined by optical density measurement (Spark, Tecan, Männedorf, Switzerland) and the approximate number of bacteria was extrapolated from a standard curve.

CAS assay to asses siderophore quantification

Magnetospirillum magneticum AMB-1 were cultured in 1.7 mL phenol red-free DMEM (11054020, Invitrogen, Carlsbad, California, USA) supplemented with GlutaMAX (35050061, Invitrogen, Carlsbad, California, USA) in a sealed 1.5 mL Eppendorf tube at 37°C for 24 h. FBS was excluded from the media and replaced with a known concentration of iron source; 25 µM holo-transferrin (T0665, Sigma-Aldrich, St. Louis, Missouri, USA). Quantification of siderophores produced by AMB-1 was performed using the Chrome Azurol S (CAS) assay (199532, Sigma-Aldrich, St. Louis, Missouri, USA).[34] 100 µL of each sample's supernatant was collected and mixed with 100 µL CAS assay solution on a transparent 96-well plate. The assay was then incubated in the dark at room temperature for 1 h before the absorbance

was measured at 630 nm on a multimode microplate reader (Spark, Tecan, Männedorf, Switzerland). The measurement was expressed in siderophore production unit (s.p.u.), which was calculated as follows:

$$\text{Siderophore production unit (s. p. u.)} = \frac{\text{OD}_{630,\text{ref}} - \text{OD}_{630}}{\text{OD}_{630,\text{ref}}}$$

DMEM supplemented with different concentrations of deferoxamine mesylate salt (DFO, D9533, Sigma-Aldrich, St. Louis, Missouri, USA) was prepared by serial dilution and used to generate a calibration curve (Supplementary 1).

Analysis of human transferrin using SDS-PAGE Electrophoresis

AMB-1 bacteria (1 x 10^8 cells/mL) were cultured in 1.7 mL phenol red-free DMEM (11054020, Invitrogen, Carlsbad, California, USA) in a sealed 1.5 mL Eppendorf tube at 30°C for 48 h. Excess volume was used to ensure no or minimal air was trapped in the tubes. 25 µM holo-transferrin (holo-Tf, T4132, Sigma-Aldrich, St. Louis, Missouri, USA), or 25 µM apo-transferrin (apo-Tf, T2036, Sigma-Aldrich, St. Louis, Missouri, USA) respectively were added to the mammalian cell culture media. Changes in transferrin molecular mass during the growth of AMB-1 were evaluated by sodium dodecyl sulfate-polyacrylamide gel electrophoresis (SDS-PAGE) analysis of culture supernatant. Electrophoresis was conducted using the protocol described by Laemmli[35] and protein loading of each sample was normalized to 2 µg. Proteins were visualized using SYPRO ruby protein stain (1703126, Bio-rad, Hercules, California, USA). The electrophoresis chamber and the reagents were purchased from Bio-rad. Stained gels were imaged using a fluorescent scanner (Sapphire Biomolecular Imager, Azure Biosystems, Dublin, California, USA) at 488 nm excitation and 658 nm emission.

Mammalian cell culture

Human melanoma MDA-MB-435S cells (ATCC, Manassas, Virginia, USA) were cultured in high glucose Dulbecco's Modified Eagle's Medium (DMEM, Invitrogen, Carlsbad, California, USA) supplemented with 10% fetal bovine serum (FBS, Biowest, Nuaille, France) and 1% penicillin-streptomycin (CellGro, Corning, New York, USA). All cells were incubated at 37°C in a humidified atmosphere with 5% CO_2 at 37°C.

Co-culture of mammalian cancer cells with magnetotactic bacteria

Human melanoma MDA-MB-435 cells (1 x 10^5 cells) were cultured on 12-well plates and incubated in a 5% CO_2 incubator at 37°C for 24 h. For microscopic analysis at high magnification (> 40x), a circular cover slip was placed in each well prior to cell seeding. Following incubation, *Magnetospirillum magneticum* AMB-1 (1 x 10^6 – 1 x 10^8 cells) were introduced into the wells. The well plate was stored in a sealable bag and the bag was flushed with nitrogen for 15 min in order to produce hypoxic conditions. The setup with the 12-well plate was then incubated at 37°C for 48 h. To serve as negative

and positive controls, 0, 10 µM and 25 µM of the iron-chelating agent deferoxamine mesylate (D9533, Sigma-Aldrich, St. Louis, Missouri, USA) was added to the MDA-MB-435S cell culture in place of AMB-1 bacteria.

Immunofluorescence labelling of MDA-MB-435S cells

After the co-culture, cells were washed with ice cold 1X Dulbecco's Phosphate-Buffered Saline solution (DPBS, Gibco, Carlsbad, California, USA) and then blocked with a 1% Bovine Serum Albumin (BSA, Sigma-Aldrich, St. Louis, Missouri, USA) solution diluted in 1X DPBS. The cells were then incubated with 10 µg/mL primary anti-TfR1 antibody (ab84036, Abcam, Cambridge, UK) on ice in dark for one h. Subsequently, the cells were washed with ice-cold DPBS and incubated with 20 µg/mL secondary goat anti-rabbit antibody (ab150077, Abcam, Cambridge, UK) and 25 µg/mL Hoechst 33342 (H3570, Thermo Fisher Scientific, Waltham, Massachusetts, USA) on ice in dark for another hour. Next, the cells were washed with ice-cold 1X PBS twice and fixed with a 2% paraformaldehyde (PFA) solution. Fixed cells were washed three times with 1X DPBS and the cover slips were mounted on glass slides and stored overnight in dark at 4°C. A Nikon Eclipse Ti2 microscope equipped with a Yokogawa CSU-W1 Confocal Scanner Unit and Hamamatsu C13440-20CU ORCA Flash 4.0 V3 Digital CMOS camera were used for visualization. Microscope operation and image acquisition was performed using Nikon NIS-Elements Advanced Research 5.02 (Build 1266) software. ImageJ v2.0 (NIH) was used to process the obtained images.

Evaluation of fluorescently labelled MDA-MB-435S cells by flow cytometry

Flow cytometry was used to measure the expression of fluorescently labelled TfR1 on the surface of MDA-MB-435S cells. Cells were harvested at different timepoints during co-culture (0h, 6h, 12h, 24h) and washed in cold 1X DPBS (Gibco Carlsbad, California, USA). Harvested cells were stained with primary anti-TfR1 antibody (ab84036, Abcam, Cambridge, UK) at a concentration of 10 µg/mL. After 1 h of incubation on ice, cells were washed twice with 1X DPBS and then stained with 20 µg/mL secondary goat anti-rabbit antibody (ab150077, Abcam, Cambridge, UK). Finally, cells were washed twice with 1X DPBS and analyzed by flow cytometry with BD LSRFortessa (BD Biosciences, San Jose, California, USA) using a 488nm excitation laser and 530/30 and 690/50 band pass emission filters for detection. FlowJo™ (Tree Star) software was used to evaluate the data.

Flow cytometry was used to assess the cell membrane integrity of MDA-MB-435S cells. Cells were harvested at different timepoints during co-culture (0h, 6h, 24h) and washed in cold 1X DPBS. Collected cells were stained with 1 µg/mL Propidium Iodide (V13242, Thermo Fisher Scientific, Waltham, Massachusetts, USA) and incubated for 30 in a humidified atmosphere with 5% CO_2 at 37°C. Finally, cells were washed twice with 1X DPBS and analyzed by flow cytometry with BD LSRFortessa (BD Biosciences, San Jose, California, USA) using a 488nm excitation laser and 610/10 bandpass emission

filters for detection. FlowJo™ (Tree Star) software was used to evaluate data and graphs were plotted using Prism 8.0 (GraphPad).

Statistics and data analysis

All graphs and statistical analyses were generated using Prism 8.0 (GraphPad). Statistical significance and number of replicates of the experiments are described in each figure and figure legend. Error bars, where present, indicate the standard error of the mean (SD). P values are categorized as * P<0.05, ** P<0.01, and *** P<0.001.

Figure Legends

Figure 1: Quantification of siderophores produced by *Magnetospirillum magneticum* AMB-1 and analysis of their interaction with human transferrin. **(A)** Siderophores produced by AMB-1 were quantified by a chrome azurol S (CAS) assay in DMEM and DMEM supplemented with 25 µM holo-transferrin (n=4 per group, statistical significance was assessed with an unpaired two-tailed *t*-test). **(B)** Siderophore production units plotted in terms of the inferred equivalent concentration of deferoxamine (n=4 per group, statistical significance was assessed with an unpaired two-tailed *t*-test). **(C)** SDS-PAGE analysis displaying the effect of AMB-1 on the structure of human transferrin. Tested conditions are indicated in the figure, with holo-Tf corresponding to saturated transferrin and apo-Tf corresponding to non-saturated transferrin.

Figure 2: Analysis of TfR1 upregulation and cell surface expression on MDA-MB-435S. **(A)** Representative immunofluorescence images of human melanoma cells co-cultured under hypoxic conditions for 48 h with different ratios of AMB-1 bacteria and different concentrations of deferoxamine as a positive control. Images show MDA-MB-435S cells marked by anti-TfR1 antibody (green) and Hoechst 33342 (blue), (scale bar: 10 µM). **(B)** Quantification of the fold change in fluorescence intensity relative to the control condition, (n=2 per condition, statistical significance was assessed with an unpaired two-tailed *t*-test). **(C)** Membrane integrity was measured as a graphical representation of PI negative and PI positive cell populations after 0, 6 and 24 h. **(D)** TfR1 median fluorescence intensity measured over 24 hours, (n=3 per timepoint, statistical significance was assessed with an unpaired two-tailed *t*-test). **(E)** Representative lognormal fitted fluorescence intensity histograms of cell surface TfR1 expression on MDA-MB-435S cells in co-culture model and **(F)** negative control, (n=3 per timepoint).

Supplementary Figure 1: Calibration curve representing the siderophore production unit plotted against the concentration of deferoxamine (n= 3).

Supplementary Figure 2: Comparison of *in vitro* cancer cell culture under either hypoxic or normoxic conditions. Representative fluorescence and brightfield images of MDA-MB-435S cells stained with Image-IT Green Hypoxia Reagent (green), (scale bar: 25 μM).

Acknowledgements

The authors thank Cameron Moshfegh for helpful discussions. Technical support was provided by the Flow Cytometry Core Facility at ETH Zurich for flow cytometry measurements. The authors appreciate the help of Nima Mirkhani with AMB-1 cultures. The authors thank Guy Riddihough (Life Science Editors) for his editing support and Michael G. Christiansen for critically reviewing the manuscript and for his support in creating the hypoxia device. SS gratefully acknowledges the support provided through the Branco Weiss Fellowship-Society in Science (title: “Cancer-fighting magnetic biobots: Harnessing the power of synthetic biology and magnetism”).

Competing interests

The authors declare no conflict of interest.

References

1. Richardson, D. R.; Ponka, P., The molecular mechanisms of the metabolism and transport of iron in normal and neoplastic cells. *Biochimica et Biophysica Acta (BBA) - Reviews on Biomembranes* **1997,** *1331* (1), 1-40.
2. Lieu, P. T.; Heiskala, M.; Peterson, P. A.; Yang, Y., The roles of iron in health and disease. *Molecular Aspects of Medicine* **2001,** *22* (1), 1-87.
3. Wang, Y.; Yu, L.; Ding, J.; Chen, Y., Iron Metabolism in Cancer. *Int J Mol Sci* **2018,** *20* (1), 95.
4. Torti, S. V.; Torti, F. M., Iron and cancer: more ore to be mined. *Nature Reviews Cancer* **2013,** *13* (5), 342-355.
5. Lane, D. J. R.; Merlot, A. M.; Huang, M. L. H.; Bae, D. H.; Jansson, P. J.; Sahni, S.; Kalinowski, D. S.; Richardson, D. R., Cellular iron uptake, trafficking and metabolism: Key molecules and mechanisms and their roles in disease. *Biochimica et Biophysica Acta (BBA) - Molecular Cell Research* **2015,** *1853* (5), 1130-1144.
6. Steegmann-Olmedillas, J. L., The role of iron in tumour cell proliferation. *Clinical and Translational Oncology* **2011,** *13* (2), 71-76.
7. Holden, V. I.; Bachman, M. A., Diverging roles of bacterial siderophores during infection. *Metallomics* **2015,** *7* (6), 986-995.
8. Wilson, B. R.; Bogdan, A. R.; Miyazawa, M.; Hashimoto, K.; Tsuji, Y., Siderophores in Iron Metabolism: From Mechanism to Therapy Potential. *Trends in Molecular Medicine* **2016,** *22* (12), 1077-1090.
9. Brittenham, G. M.; Griffith, P. M.; Nienhuis, A. W.; McLaren, C. E.; Young, N. S.; Tucker, E. E.; Allen, C. J.; Farrell, D. E.; Harris, J. W., Efficacy of Deferoxamine in Preventing Complications of Iron Overload in Patients with Thalassemia Major. *New England Journal of Medicine* **1994,** *331* (9), 567-573.

10. Mobarra, N.; Shanaki, M.; Ehteram, H.; Nasiri, H.; Sahmani, M.; Saeidi, M.; Goudarzi, M.; Pourkarim, H.; Azad, M., A Review on Iron Chelators in Treatment of Iron Overload Syndromes. *Int J Hematol Oncol Stem Cell Res* **2016,** *10* (4), 239-247.
11. Hatcher, H. C.; Singh, R. N.; Torti, F. M.; Torti, S. V., Synthetic and natural iron chelators: therapeutic potential and clinical use. *Future Med Chem* **2009,** *1* (9), 1643-1670.
12. Bedford, M. R.; Ford, S. J.; Horniblow, R. D.; Iqbal, T. H.; Tselepis, C., Iron Chelation in the Treatment of Cancer: A New Role for Deferasirox? *The Journal of Clinical Pharmacology* **2013,** *53* (9), 885-891.
13. Ford, S. J.; Obeidy, P.; Lovejoy, D. B.; Bedford, M.; Nichols, L.; Chadwick, C.; Tucker, O.; Lui, G. Y. L.; Kalinowski, D. S.; Jansson, P. J.; Iqbal, T. H.; Alderson, D.; Richardson, D. R.; Tselepis, C., Deferasirox (ICL670A) effectively inhibits oesophageal cancer growth in vitro and in vivo. *Br J Pharmacol* **2013,** *168* (6), 1316-1328.
14. Lui, G. Y. L.; Obeidy, P.; Ford, S. J.; Tselepis, C.; Sharp, D. M.; Jansson, P. J.; Kalinowski, D. S.; Kovacevic, Z.; Lovejoy, D. B.; Richardson, D. R., The Iron Chelator, Deferasirox, as a Novel Strategy for Cancer Treatment: Oral Activity Against Human Lung Tumor Xenografts and Molecular Mechanism of Action. *Molecular Pharmacology* **2013,** *83* (1), 179.
15. Richardson, D. R., Iron chelators as therapeutic agents for the treatment of cancer. *Critical Reviews in Oncology/Hematology* **2002,** *42* (3), 267-281.
16. Yu, Y.; Gutierrez, E.; Kovacevic, Z.; Saletta, F.; Obeidy, P.; Rahmanto, Y. S.; Richardson, D. R., Iron Chelators for the Treatment of Cancer. *Current Medicinal Chemistry* **2012,** *19* (17), 2689-2702.
17. Saha, P.; Yeoh, B. S.; Xiao, X.; Golonka, R. M.; Kumarasamy, S.; Vijay-Kumar, M., Enterobactin, an iron chelating bacterial siderophore, arrests cancer cell proliferation. *Biochemical Pharmacology* **2019,** *168*, 71-81.
18. Mirabello, G.; Lenders, J. J. M.; Sommerdijk, N. A. J. M., Bioinspired synthesis of magnetite nanoparticles. *Chemical Society Reviews* **2016,** *45* (18), 5085-5106.
19. Faivre, D.; Schüler, D., Magnetotactic Bacteria and Magnetosomes. *Chemical Reviews* **2008,** *108* (11), 4875-4898.
20. Bazylinski, D.; Williams, T., Ecophysiology of Magnetotactic Bacteria. 1970; pp 37-75.
21. Yan, L.; Zhang, S.; Chen, P.; Liu, H.; Yin, H.; Li, H., Magnetotactic bacteria, magnetosomes and their application. *Microbiological Research* **2012,** *167* (9), 507-519.
22. González, L. M.; Ruder, W. C.; Mitchell, A. P.; Messner, W. C.; LeDuc, P. R., Sudden motility reversal indicates sensing of magnetic field gradients in Magnetospirillum magneticum AMB-1 strain. *The ISME Journal* **2015,** *9* (6), 1399-1409.
23. Lefèvre, C. T.; Bennet, M.; Landau, L.; Vach, P.; Pignol, D.; Bazylinski, D. A.; Frankel, R. B.; Klumpp, S.; Faivre, D., Diversity of magneto-aerotactic behaviors and oxygen sensing mechanisms in cultured magnetotactic bacteria. *Biophys J* **2014,** *107* (2), 527-538.
24. Felfoul, O.; Mohammadi, M.; Taherkhani, S.; de Lanauze, D.; Zhong Xu, Y.; Loghin, D.; Essa, S.; Jancik, S.; Houle, D.; Lafleur, M.; Gaboury, L.; Tabrizian, M.; Kaou, N.; Atkin, M.; Vuong, T.; Batist, G.; Beauchemin, N.; Radzioch, D.; Martel, S., Magneto-aerotactic bacteria deliver drug-containing nanoliposomes to tumour hypoxic regions. *Nature Nanotechnology* **2016,** *11*, 941.
25. Mengesha, A.; Dubois, L.; Lambin, P.; Landuyt, W.; Chiu, R. K.; Wouters, B. G.; Theys, J., Development of a flexible and potent hypoxia-inducible promoter for tumor-targeted gene expression in attenuated salmonella. *Cancer Biology & Therapy* **2006,** *5* (9), 1120-1128.
26. Yu, B.; Yang, M.; Shi, L.; Yao, Y.; Jiang, Q.; Li, X.; Tang, L.-H.; Zheng, B.-J.; Yuen, K.-Y.; Smith, D. K.; Song, E.; Huang, J.-D., Explicit hypoxia targeting with tumor suppression by creating an “obligate” anaerobic Salmonella Typhimurium strain. *Scientific Reports* **2012,** *2* (1), 436.

27. Din, M. O.; Danino, T.; Prindle, A.; Skalak, M.; Selimkhanov, J.; Allen, K.; Julio, E.; Atolia, E.; Tsimring, L. S.; Bhatia, S. N.; Hasty, J., Synchronized cycles of bacterial lysis for in vivo delivery. *Nature* **2016,** *536*, 81.
28. Chowdhury, S.; Castro, S.; Coker, C.; Hinchliffe, T. E.; Arpaia, N.; Danino, T., Programmable bacteria induce durable tumor regression and systemic antitumor immunity. *Nature Medicine* **2019,** *25* (7), 1057-1063.
29. Forbes, N. S., Engineering the perfect (bacterial) cancer therapy. *Nature Reviews Cancer* **2010,** *10* (11), 785-794.
30. Duong, M. T.-Q.; Qin, Y.; You, S.-H.; Min, J.-J., Bacteria-cancer interactions: bacteria-based cancer therapy. *Experimental & Molecular Medicine* **2019,** *51* (12), 152.
31. Calugay, R. J.; Miyashita, H.; Okamura, Y.; Matsunaga, T., Siderophore production by the magnetic bacterium Magnetospirillum magneticum AMB-1. *FEMS Microbiology Letters* **2003,** *218* (2), 371-375.
32. Duchesne, P.; Grenier, D.; Mayrand, D., Binding and utilization of human transferrin by Prevotella nigrescens. *Infect Immun* **1999,** *67* (2), 576-580.
33. Bajbouj, K.; Shafarin, J.; Hamad, M., High-Dose Deferoxamine Treatment Disrupts Intracellular Iron Homeostasis, Reduces Growth, and Induces Apoptosis in Metastatic and Nonmetastatic Breast Cancer Cell Lines. *Technol Cancer Res Treat* **2018,** *17*, 1533033818764470-1533033818764470.
34. Schwyn, B.; Neilands, J. B., Universal chemical assay for the detection and determination of siderophores. *Analytical Biochemistry* **1987,** *160* (1), 47-56.
35. Laemmli, U. K., Cleavage of Structural Proteins during the Assembly of the Head of Bacteriophage T4. *Nature* **1970,** *227* (5259), 680-685.

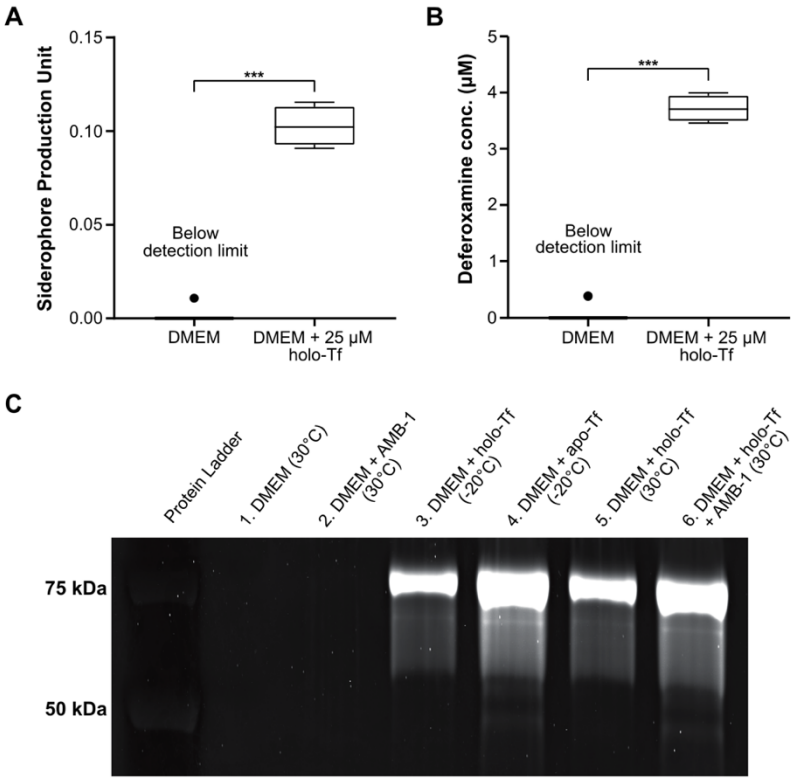

Figure 1

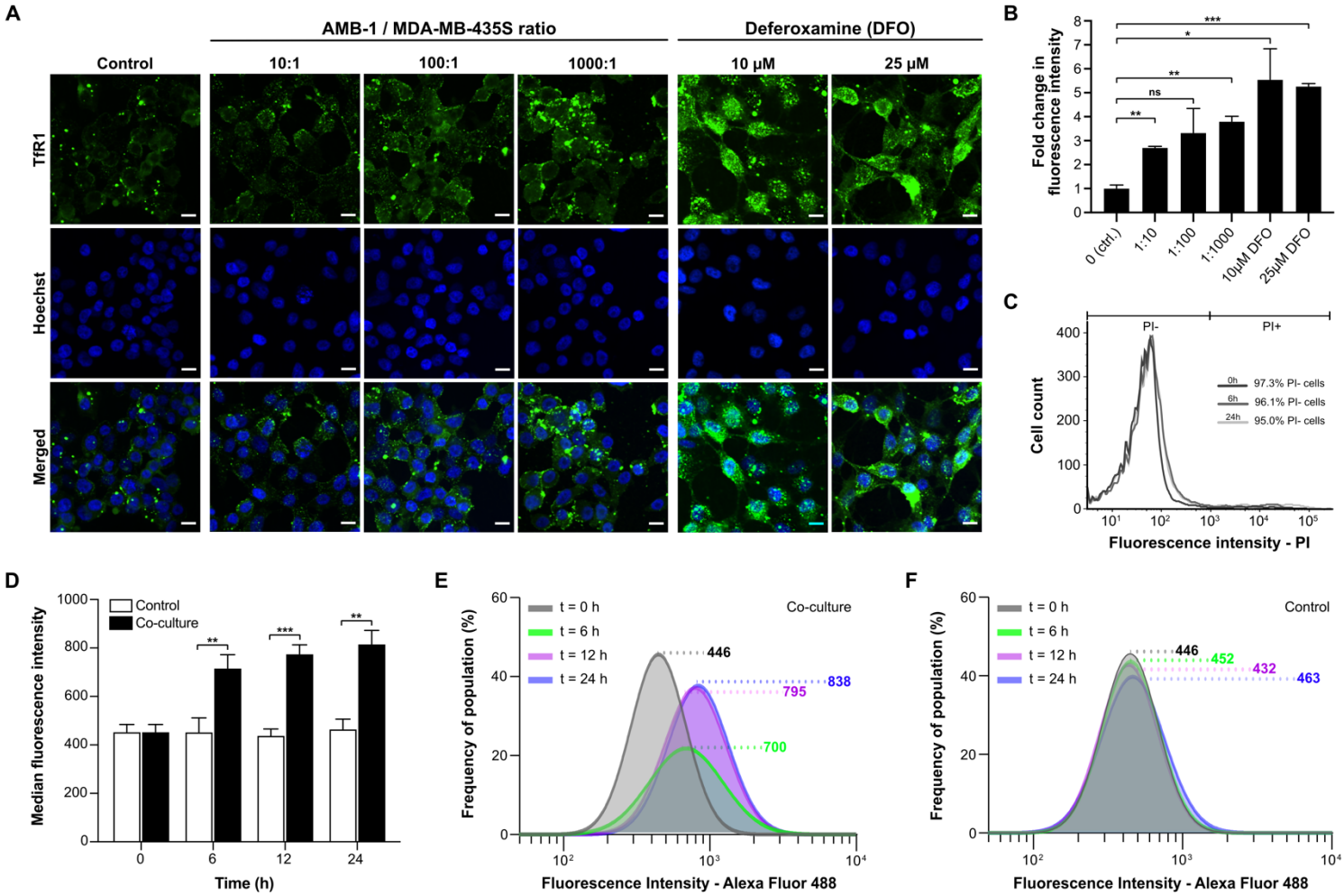

Figure 2

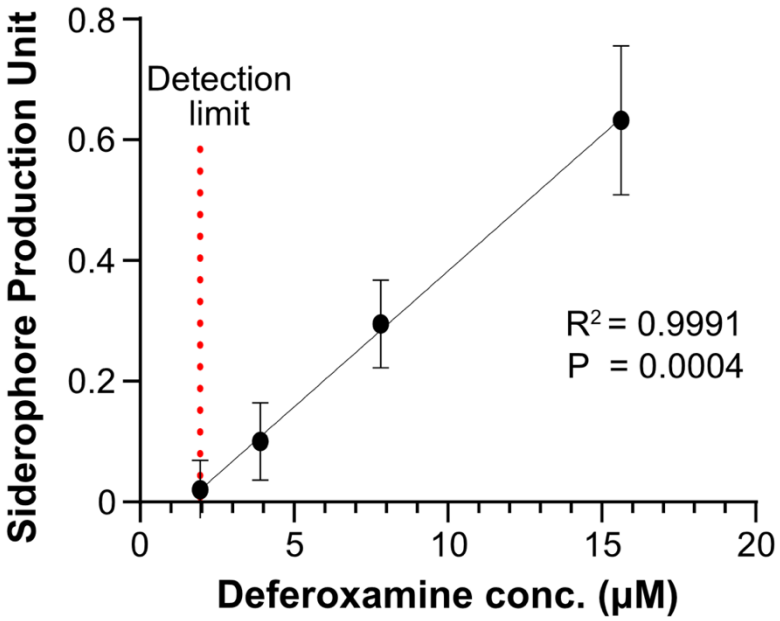

Supplementary 1

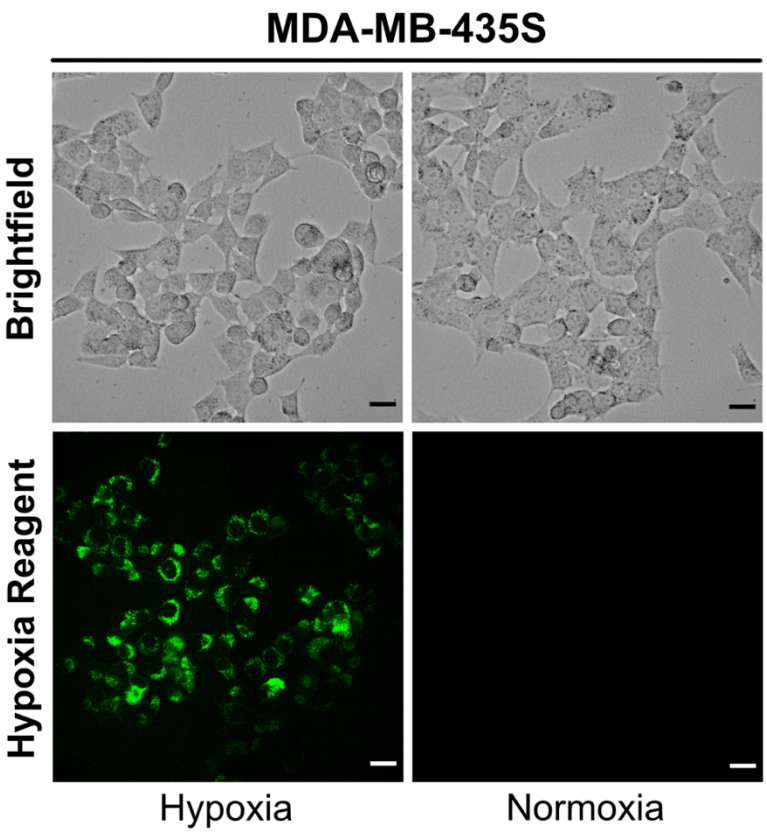

Supplementary 2